Foot and Ankle Surgery 25 (2019) 739–747

Contents lists available at ScienceDirect

Foot and Ankle Surgery

journal homepage: www.elsevier.com/locate/fas

Metal artifact reduction MRI for total ankle replacement sagittal balance evaluation

Cesar de Cesar Netto[a,b,c,*], Lew C. Schon[b], Lucas Furtado da Fonseca[b], Apisan Chinanuvathana[a,b], Steven E. Stern[d], Jan Fritz[a]

[a] Russell H. Morgan Department of Radiology and Radiological Science, Johns Hopkins University School of Medicine, 601 North Caroline Street, Baltimore, MD 21287, USA
[b] Department of Orthopaedic Surgery, Medstar Union Memorial Hospital, 201 E University Pkwy, Baltimore, MD 21218, USA
[c] Department of Foot and Ankle Surgery, Hospital for Special Surgery, 535 East 70th Street, New York, NY 10021, USA
[d] Bond Business School, Bond University, Gold Coast, QLD 4229, Australia

ARTICLE INFO

Article history:
Received 24 February 2018
Received in revised form 23 August 2018
Accepted 26 September 2018

Keywords:
Total ankle replacement
Total ankle arthroplasty
Sagittal balance
MRI
Metal artifact reduction

ABSTRACT

Background: Restoration of anatomical relationship between talus and tibia is crucial for longevity of total ankle replacement (TAR). Weight-bearing (WB) radiographs are the standard for evaluating the sagittal balance alignment, but are prone to rotational misalignment and altered measurements. Metal artifact reduction sequence (MARS) MRI allows visualization of periprosthetic landmarks and alignment of the image plane to the true sagittal axis of the implant. The purpose of this study was to compare TAR sagittal balance measurements on MARS MRI and WB radiographs.
Methods: Twenty-three subjects with TAR [10 men/13 women, age 60 (41–73) years; 13 (3–24) months post-op] underwent MARS MRI and standard lateral WB radiographs. Standardized MARS MR images were aligned to the sagittal talar component axis. Three observers performed sagittal balance alignment measurements twice in an independent, random and blinded fashion. Lateral Talar Station (LTS), tibial axis-to-talus (T-T) ratio and normalized tibial axis-to-lateral-process (T-L) distance were measured. Concordance correlation coefficients (CCC) and intraclass correlation coefficients (ICC) were used for statistical analysis. In addition, mixed effects linear models were employed to assess overall concordance of the two image types.
Results: The intraobserver agreement was excellent for radiographic (CCC = 0.96) and MRI (CCC = 0.90–0.97) measurements. Interobserver agreements were good-to-excellent with overall slightly higher agreements for MRI (ICC = 0.78–0.94) than radiography (ICC = 0.78–0.90) measurements. The T-T ratios of radiographs and MRI showed a high degree of concordance, whereas LTS was significantly lower on MRI when compared with radiographs, and T-L distance showed notable disagreement between the two imaging types.
Conclusion: Sagittal balance measurements performed on standardized weight-bearing radiographs and standardized MARS MRI demonstrate substantial correlation and similarity. Given its high intra and interobserver agreement, MARS MRI may be helpful for the evaluation of TAR sagittal balance.
Level of evidence: Level II - Prospective Comparative Study.

1. Introduction

Osteoarthritis of the ankle may lead to anatomic misalignment and as a result to mechanical dysfunction and decreased surface contact area of the joint [1–3]. Although deformities can occur both in the sagittal and coronal plane, sagittal plane deformities are most common and seem to alter the joint mechanics to a greater degree [1,2,4,5]. Total ankle replacement (TAR) has the ability for restoration of the anatomic sagittal alignment [6,7], which accordingly has been found to be an important factor for good long-term replaced patients [8–12].

In order to accurately assess the sagittal alignment of implants, the exact definition of the true sagittal axis of the distal tibia and the location of the talus in relation to this axis are required. Lateral weight-bearing radiographs are commonly used for this assessment; however, due to the projectional nature of radiographs, sagittal alignment measurements may be substantially altered by

* Corresponding author at: Hospital for Special Surgery, 535 E 70th Street, New York, NY 10021, USA.
E-mail address: cesardecesarnetto@gmail.com (C. de Cesar Netto).

https://doi.org/10.1016/j.fas.2018.09.005

even small variations of ankle positioning, especially with rotational misalignment [13].

Modern metal artifact reduction sequence (MARS) magnetic resonance imaging (MRI) techniques results in near complete elimination of implant-induced metal artifacts and geometric distortions that previously obscured relevant anatomic landmarks [14,15]. Although acquired without weight-bearing, the use of a boot-shaped imaging coil allows for standardized neutral ankle positioning during the MRI exam. Furthermore, MRI allows for the alignment of image planes in parallel to the true sagittal plane of the ankle, which seems a favorable prerequisite for sagittal alignment assessments.

The purpose of this study was to test the hypothesis that MARS MRI can be used for the assessment of sagittal balance alignment following TAR and produces at least similarly accurate measurements when compared to lateral WB radiographs.

2. Material and methods

Institutional review board approval was obtained for this prospective dual-center study. Written informed consent was obtained from all participants.

2.1. Study design

Patients were prospectively recruited between 2014 and 2016 through our tertiary hospital clinic. Enrollment criteria were history of a TAR, adult age, absence of symptoms, agreement to cooperate. Exclusion criteria included severe claustrophobia, inability of supine positioning, and the standard contraindications for MRI. All patients were screened, enrolled, and included in accordance with the CONSORT guidelines.

2.2. Subjects

A total of 60 subjects were evaluated, of which 23 patients (10 men, 13 women; 10 left and 13 right TAR; mean age of 62, range 42–75) with 23 TAR were included (Fig. 1).

All subjects completed radiography and MARS MRI exams of the replaced ankle within 60 days. The average age at time of TAR surgery was 60 years of age (range, 41–73 years of age) and the average BMI was of 29.27 kg/m^2 (range, 21.03–41.15 kg/m^2). Imaging studies were obtained at an average of 13 months (range, 3–24 months) following TAR.

2.3. Radiography technique

Weight-bearing lateral ankle radiographs of the replaced ankles were obtained using non-mobile digital radiography units (Multix Select DR, Siemens Healthcare, Erlangen, Germany) following the same strict protocol for adequate positioning of the ankle during image acquisition in all subjects. A source-to-image receptor distance of 40 in. was used. The center of the x-ray beam aimed at the ankle joint, which was kept in neutral position. The foot and ankle was positioned in 10° of internal rotation so that the malleoli were co-aligned along the X-ray beam. The distal 15 cm of the tibia were included in the field-of-view.

2.4. MRI technique

All MRI studies were performed on a commercially available 1.5 Tesla MRI system and a commercially available boot-shaped ankle coil (Magnetom Aera, Siemens Healthcare), which afforded standardized ankle neutral positioning. The MARS MRI protocol included initial scout sequences and an 8-fold accelerated sagittal intermediate-weighted slice-encoding metal artifact correction (SEMAC) turbo spin echo pulse sequence with 3 mm slice thickness and 0.5×0.5 mm^2 pixel size [14]. Accelerated SEMAC is an advanced metal artifact reduction technique that is especially suited to reduce large metal artifacts and image distortions of cobalt-containing implants [16]. During post-processing, multiple sagittal MARS MR images were transformed into a single image using standard maximum intensity projection technique. This resulted in the inclusion of all anatomic landmarks into one single image, resembling a lateral ankle radiographic view.

2.5. Measurements

Image annotations were removed after which the studies were randomized and assigned a unique number to ensure blinded assessments. Images were digitally transferred into a dedicated software (Medstrat, Echoes, Downers Grove, Illinois/US) for computer-based measurements. Following completion of a mentored training period in which readers learnt the software and measurements, three board-certified foot ankle surgeons performed the sagittal alignment measurements in an independent fashion. Each observer performed a second set of measurements following a wash-out period of 1 month after the first assessment was completed.

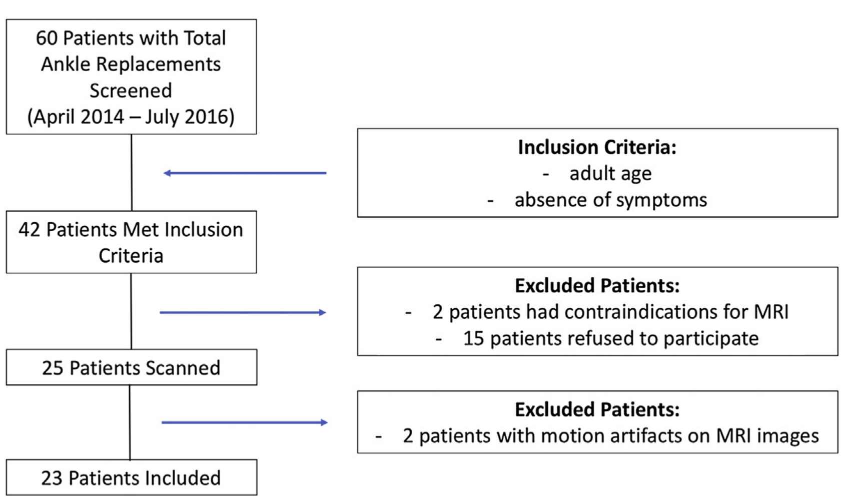

Fig. 1. CONSORT diagram of screened, enrolled, and included patients.

Measurements were performed in accordance ankle joint sagittal balance evaluation technique described by Tochigi et al. [13] both on radiographs and MRI. Initially, three talar anatomical landmarks were determined (Fig. 2): point A or posterior talar point; point B, the vertical projection of the most anterior aspect of the talus; point C represented the tip of the lateral talar process. The length of the line connecting points A and B was defined as the longitudinal talar length (AB) (Fig. 3). In the tibia, two circles were made to fit the anterior and posterior tibial shaft cortices, as described by Barg et al. [6]. The circles were positioned at approximately 5 and 10 cm above the ankle joint line [13]. The longitudinal line intersecting the center of the two circles was defined as the distal tibial axis (DTA) (Fig. 4).

We then calculated the Tibial-axis-to-Talus ratio (T-T ratio) [%], Tibial-axis-to-Lateral Process Distance (T-L distance) (Fig. 5), Tibial-axis-to-Lateral process ratio (T-L ratio), as defined by Tochigi et al. [13] and the Lateral Talar Station (LTS), as defined by Veljkovic et al. [17] (Fig. 6).

2.6. Statistical analysis

Measurement repeatability of LTS, T-T and T-L ratios was assessed with Lin's concordance correlation coefficient (CCC) with 95% confidence interval (CI). A concordance correlation coefficient of less than 0.9 was considered poor, 0.90–0.95 moderate, 0.95–0.99 substantial, and greater than 0.99 almost perfect agreement. In addition, Bland–Altman plots were computed of each of the measurements on each of the image types. Inter-reader reliability was assessed with intra-class correlation coefficients (ICC), whereas ICCs greater than 0.9 was considered first class, 0.8–0.9 second class and 0.7–0.8 third class. In addition, we calculated the inter-class standard deviation of reader measurements as an indicator of the degree of any reader-specific biases in reading the images. Concordance of measurements on MRI and radiographs was assessed by plotting measurements against each other. Based on repeatability and reliability, the concordances of MRI and radiographs were investigated with the effects of readers and replication removed by comparing averaged measures for each patient from each image type. Further, linear mixed effects models were applied to assess reader-adjusted concordance between image types.

3. Results

Mean values for radiographic and MRI measurements are given in Table 1. The values were generally lower for MRI when compared to radiographs.

3.1. Measurement repeatability

Table 2 shows the CCC with 95% CI and 95/95 tolerance limits. There was overall substantial intraobserver agreement of LTS, T-T and T-L ratios, as indicated by high concordance and relatively low tolerance limits. T-T and T-L ratios were slightly more repeatable on MRI than on radiographs, and LTS was less repeatable on MRI than on radiographs. The Bland–Altman plots (Fig. 7) corroborate the high repeatability of the measurements.

3.2. Reader reliability

Table 3 shows the ICCs for each measurement in each image type and the inter-class standard deviation for reader measurements. There was general high inter-reader reliability. In particular, the T-T and T-L ratios measured on MRI had a very high intra-class correlation. The inter-class standard deviations of reader measurements were low, with the possible exception of the T-T ratio on radiographs.

3.3. Measure concordance

Owing to the high agreement between measurements, the effects of possible inter-reader variability were removed via averaging, and new concordance and comparability plots were created (Fig. 8). The concordance correlations suggested three distinct patterns of potential concordance of LTS, T-T and T-L ratios (Table 4), which were further investigated with linear mixed models.

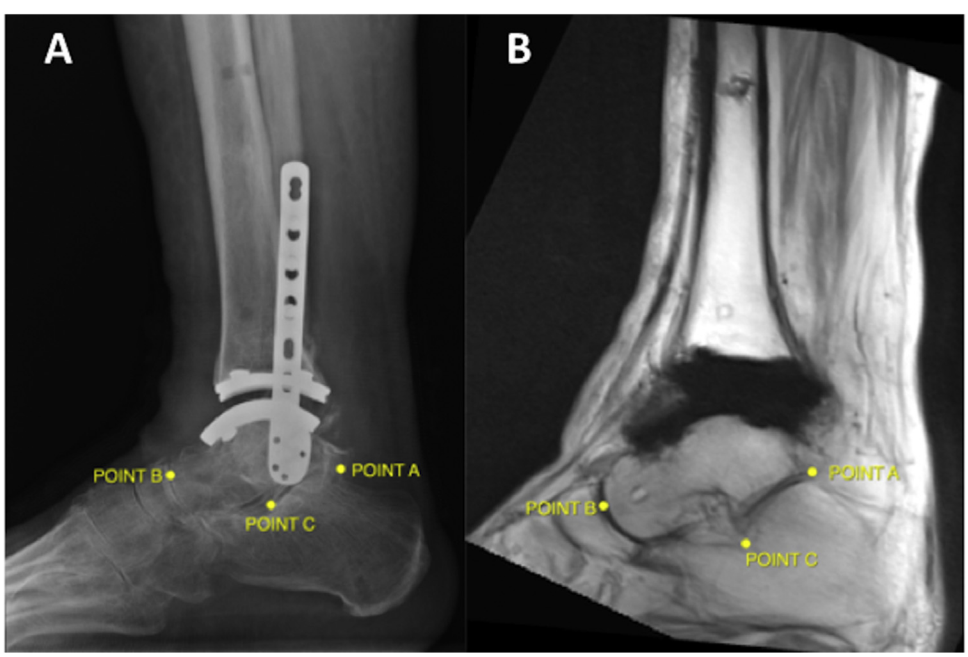

Fig. 2. Anatomical landmarks points of the talus on lateral radiograph (A) and maximum intensity projection sagittal MARS MR image (B). Point A (posterior talar point) is the intersection of the posterior subtalar articular contour and the posterosuperior contour of the calcaneus. Point B (anterior talar aspect) is the vertical projection of the most anterior aspect of the talus in the talar reference line, drawn through point A, and parallel to the floor. Point C is the tip of the lateral talar process.

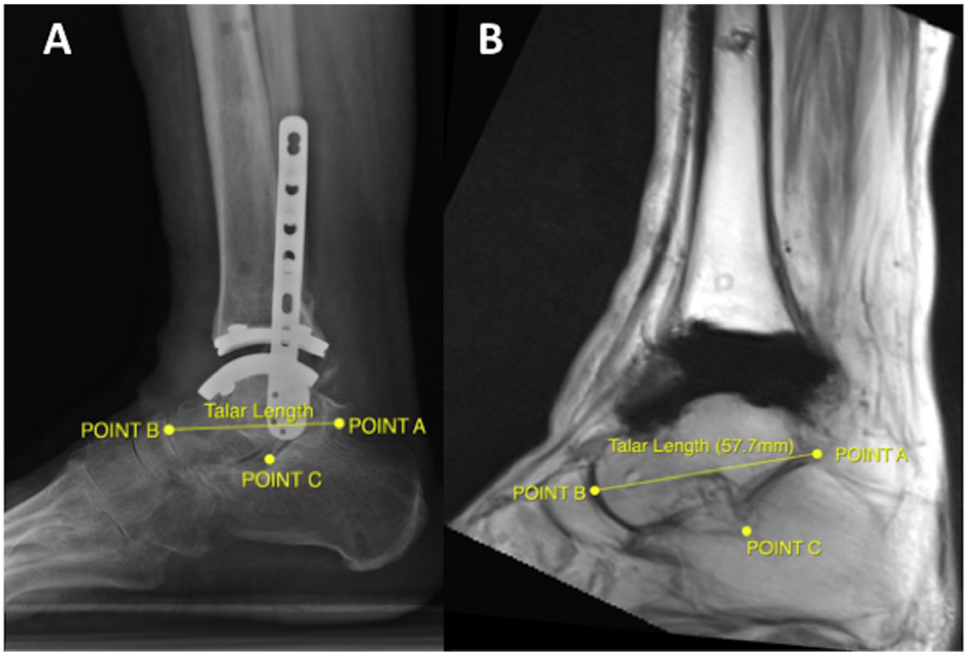

Fig. 3. Longitudinal Talar Length on lateral radiograph (A) and maximum intensity projection sagittal MARS MR image (B) connecting points A and B.

We first fit the model for the T-T ratios, which derived an intercept of 2.965 (95% CI: −1.167 to 7.097) and a slope of 0.926 (95% CI: 0.804–1.049). Because the 95% CI contained the value zero for the intercept and the value 1 for the slope, and the negligible random effect variation for intercept and slope accounting for less than 1% of the overall variation in measurements, we concluded that there is a very strong concordance between the T-T ratios of radiographs and MRI.

Next, we fit the mode for the LTS measurements, which derived an intercept of 2.730 (95% CI: 1.543–3.917) and slope of 1.010 (95% CI: 0.855–1.164). Again, the 95% CI of the slope contained the value 1 and the associated variation for slope random effects was negligible. However, the intercept CI did not contain the value zero and the random effect for reader-specific intercept effects was non-negligible accounting for about 12% of overall variation in measurements. As such, we concluded that there is reasonable

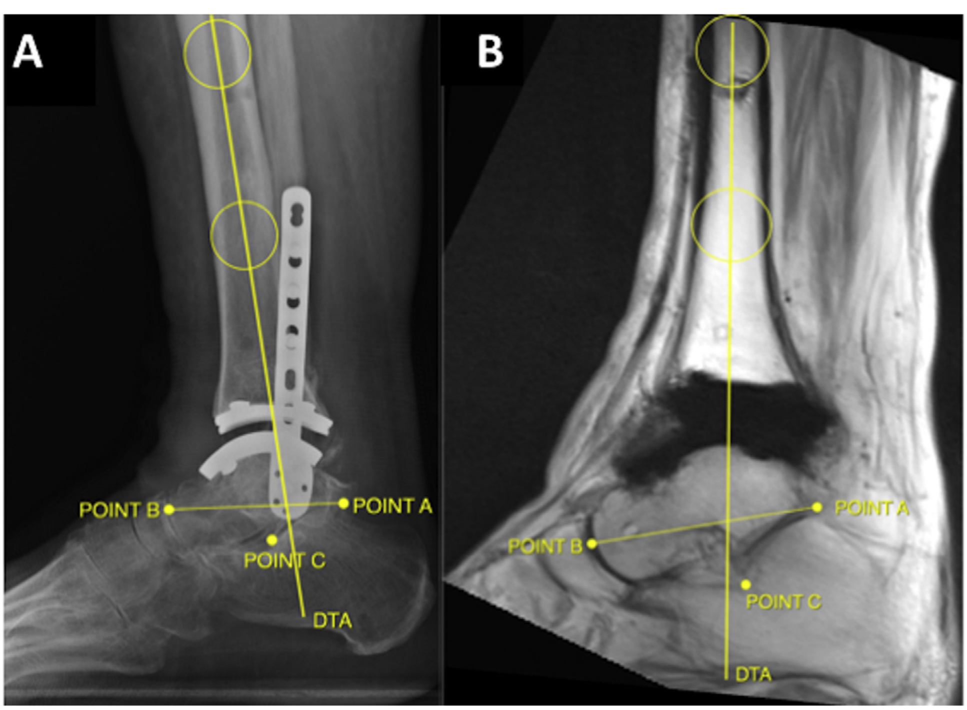

Fig. 4. Distal tibial axis (DTA) on lateral radiograph (A) and maximum intensity projection sagittal MARS MR image (B). The distal tibial axis was defined as the line bisecting the anterior and posterior surface points of the distal tibial shaft at approximately 5 and 10 cm above the ankle.

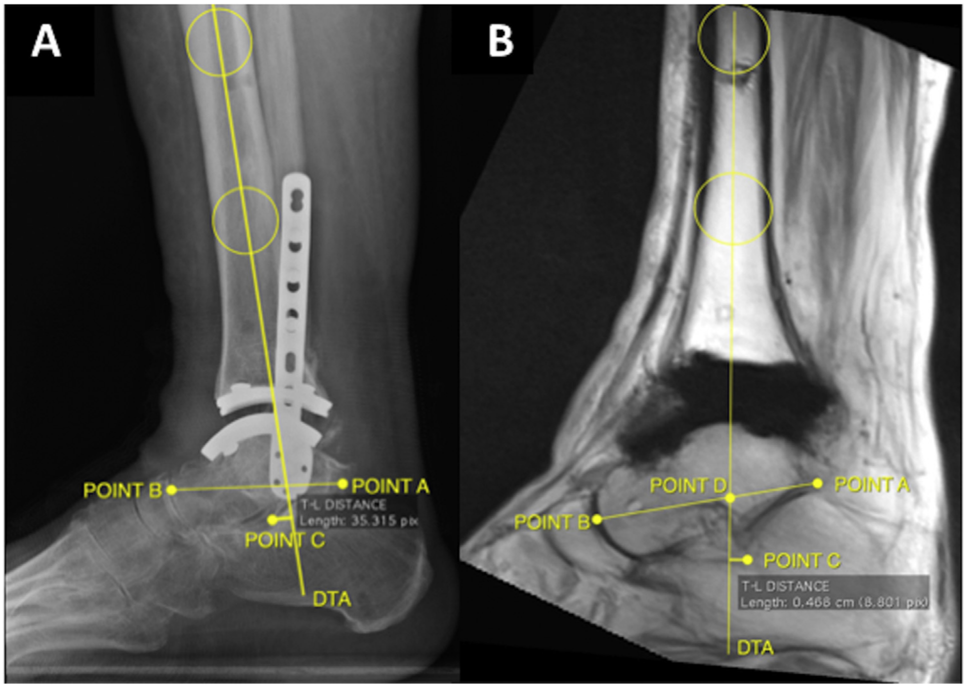

Fig. 5. Tibial-axis-to-Lateral Process distance (T-L distance) on lateral radiograph (A) and maximum intensity projection sagittal MARS MR image (B). The Tibial-axis-to-Lateral Process distance was defined as the perpendicular distance from distal tibial axis (DTA) to point C. When point C was posterior to DTA, this measurement was defined as a negative value.

relative concordance between LTS measurements from the two image types, but that a shift adjustment of 2.73 on average was necessary to bring them into full concordance.

Lastly, we fit the model for the T-L ratios, which derived an intercept of 6.376 (95% CI: 4.399–8.353) and slope of 0.838 (95% CI: 0.638–1.037). Similar to LTS measurements, the 95% CI for the slope contained the value 1, but the intercept interval did not contain the value zero. Moreover, while the random reader effects for both intercept and slope were negligible, there was clear heteroskedastic structure visible in the scatterplot of the measurements (Fig. 8), and the simple linear model structure may not be appropriate to the circumstances.

4. Discussion

To our knowledge, this is the first study to describe the use of MRI for the evaluation of ankle sagittal balance following TAR. We demonstrated the feasibility of SEMAC MARS MRI of ankle

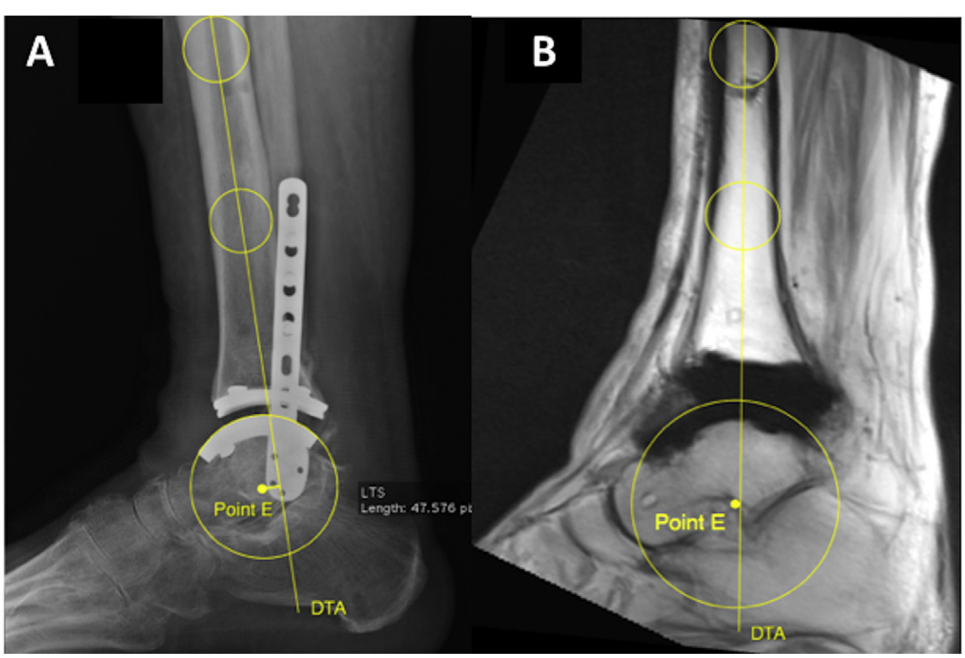

Fig. 6. Lateral Talar Station (LTS) on lateral radiograph (A) and maximum intensity projection sagittal MR image (B). The Lateral Talar Station was defined as the lateral perpendicular distance from the center (point E) of a circle fitting the talar component dome to the distal tibial axis (DTA).

Table 1
Mean values, standard deviation and standard error for radiographic and MRI sagittal balance measurements.
LTS = Lateral Talar Station (mm).
T-L Distance = Tibial-axis-to-Lateral Process Distance (mm).
T-L Ratio = Tibial-axis-to-Lateral Process Distance, normalized to the talar length (%)
Talar Length (mm).

	Mean value	Standard deviation	Standard error
LTS radiography	2.96	4.62	0.39
LTS MRI	0.22	3.93	0.33
Talar length radiography	57.99	4.75	0.40
Talar length MRI	52.44	3.83	0.33
T-L distance radiography	6.74	5.35	0.46
T-L distance MRI	3.23	4.45	0.38
T-T ratio radiography	35.00	8.47	0.72
T-T ratio MRI	34.56	7.92	0.67
T-L ratio radiography	11.57	9.17	0.78
T-L ratio MRI	6.19	7.82	0.67

T-T Ratio = Tibial-axis-to-Talus Ratio (%).
LTS = Lateral Talar Station (mm).
T-L Distance = Tibial-axis-to-Lateral Process Distance (mm).
T-L Ratio = Tibial-axis-to-Lateral Process Distance, normalized to the talar length (%)
Talar Length (mm).

arthroplasty implants for the evaluation of sagittal balance. Measurements made on MR images and lateral weight-bearing radiographs both showed high repeatability and reliability; however, measurements made on MR images were slightly more reliable and consistent. Measurements were generally lower on MR images. There was very strong inter-method concordance for the T-T ratio and for the LTS with shift correction. The T-L ratio did not demonstrate a linear relationship between measurements on MR images and lateral weight-bearing radiographs, which suggests a fundamental difference between the two techniques.

The accurate determination of the sagittal ankle alignment following arthroplasty requires an accurate and reliable definition of the sagittal distal tibial axis and the location of the talus relative to this axis. Lateral weight-bearing radiographs of the ankle are considered the standard technique for the assessment of ankle sagittal balance; however, radiographs are prone to inaccuracies due to positional malalignment. Tochigi et al. demonstrated the influence of ankle malpositioning in the transverse and sagittal planes for the sagittal balance evaluation on lateral ankle radiographs and multiple other studies have similarly addressed the difficulty in the interpretation of malrotated projections on consecutive radiographic measurements [10,13,18–23]. Radiographic parameters used to investigate ankle alignment [13,17,24,25], TAR component malalignment [10,26], subsidence [27,28], and range of motion [29–31] are substantially influenced by the rotational position of the leg during the acquisition of the radiographs. Furthermore, difficulties in reproducibly positioning the ankle for a standing radiograph in clinical practice may pose difficulties in the assessment of the components positioning and migration after TAR. The images acquired could be misinterpreted as a sign of loosening and unnecessarily leads to further imaging evaluation and even revision surgery [32,33].

The rationale for the use of MARS MRI in the evaluation of sagittal ankle alignment is based on its ability to accurately align the imaging plane along the individual longitudinal axis of the patient's ankle. Dedicated metal artifact reduction techniques can achieve near complete suppression of metal implant-induced distortion and signal voids [14]. The cross-sectional nature of MRI favorably complies with the requirement for unobscured visualization of pertinent anatomical references and landmarks and may be less prone to positional and observer variations due to the elimination of projection effects and superimposition of anatomic structures on radiography. While MARS MRI may not be obtained for the sole purpose of sagittal alignment measurements, the measurements can be performed with MR images from studies that were obtained during the work-up of symptomatic TAR [14]. The advent of weight-bearing cone beam computed tomography (CBCT) might represent an interesting weight-bearing alternative for cross-sectional imaging evaluation of TAR sagittal balance in the near future. However, in our experience, the currently available CBCT technologies still produce substantial anatomy-obscuring metal artifacts, which may interfere with the adequate evaluation of important bone landmarks.

Our results suggested that the repeated MRI measurements of the three experienced observers were slightly more reliable and consistent than radiographic measurements. We believe that the difference favoring MRI is based on the better visualization of the anatomical landmarks used for an accurate sagittal balance evaluation. Normal values for ankle sagittal balance have been proposed previously in the literature [6,13,17,34], but since the true alignment measurement values are unknown, our results do not necessarily mean that MRI is more accurate, but rather that MRI measurements are more consistent amongst readers. However, reader consistency is an important prerequisite for establishing thresholds between normal and abnormal values, for which the most consistent technique should be used.

Our study found lower values for talar length measurements on MRI when compared to radiographs. In our interpretation, the difference exemplifies the influence of the projectional nature of radiographs on measurements. Depending on the rotational position of the structure under evaluation, measured values can represent underestimates or overestimates of the true value. We believe that measurements performed on MRI are closer to the true anatomical measurements.

Similar to results of previous studies [7,13], we found excellent repeatability and reader reliability for T-T ratios. When comparing measurements done on MRI and radiographs, MRI showed slightly better consistency and repeatability. Tochigi et al. described the T-T ratio as a reliable and valid radiographic measurement of anteroposterior tibio-talar alignment with a good tolerance against perturbations of ankle positioning [13]. The high tolerance described in their study could explain the high concordance between T-T ratios of radiographs and MRI. Since one might expect

Table 2
Concordance correlation and tolerance for repeated measurements.

Measurement	Radiographs			MR images		
	Concordance		95/95 Tolerance	Concordance		95/95 Tolerance
	Correlation	95% Interval		Correlation	95% Interval	
LTS	0.963	(0.941, 0.976)	2.512	0.903	(0.849, 0.939)	3.458
T-T Ratio	0.964	(0.942, 0.977)	4.565	0.968	(0.948, 0.980)	4.020
T-L Ratio	0.963	(0.941, 0.977)	4.993	0.974	(0.959, 0.984)	3.486

LTS = Lateral Talar Station.
T-T Ratio = Tibial-axis-to-Talus Ratio.
T-L Ratio = Tibial-axis-to-Lateral Process Distance, normalized to the talar length.

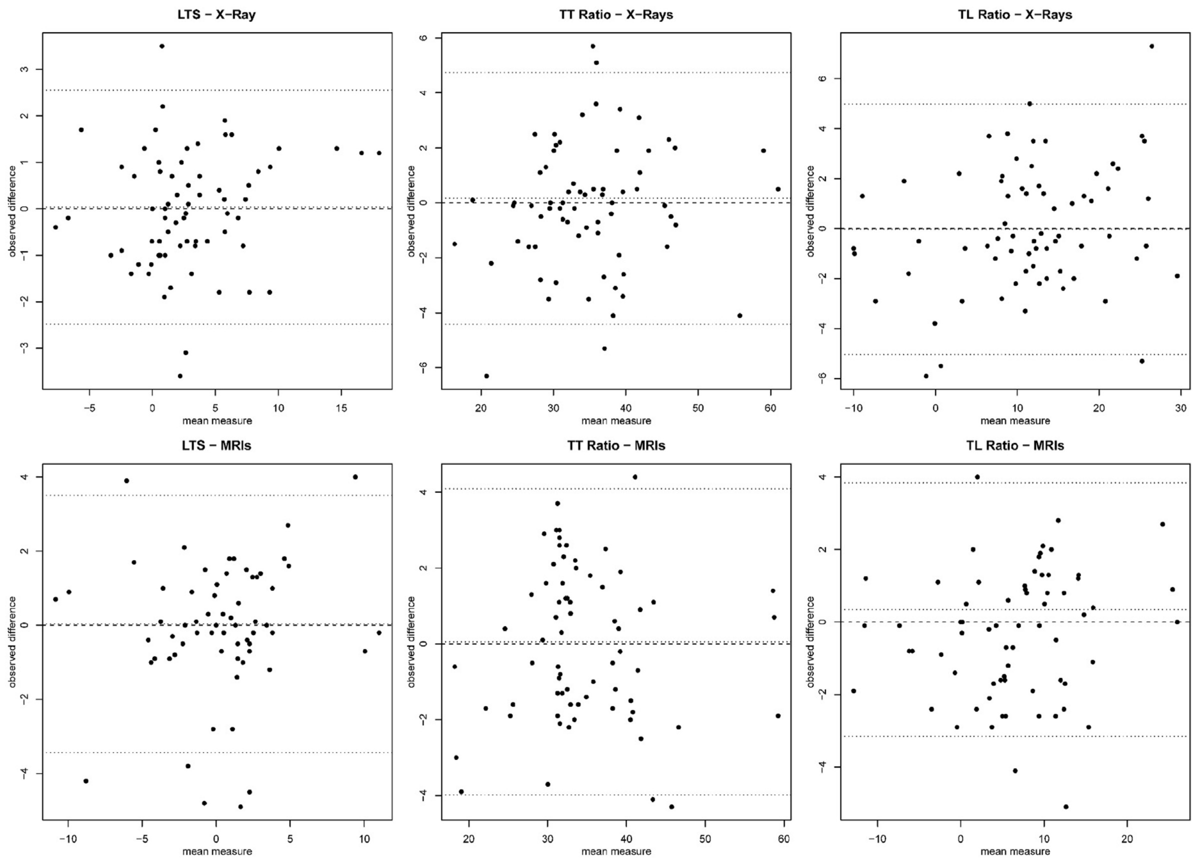

Fig. 7. Bland–Altman plots for each of the measurements on radiographic and MRI measurements. LTS = Lateral Talar Station. T-T ratio = Tibial-axis-to-Talus ratio. T-L ratio = Tibial-axis-to-Lateral Process distance, normalized to the talar length.

a higher variation of the sagittal and transverse positioning of the ankle on radiographs than on MRI, the similar results found may be interpreted as a reflection of the capacity of the T-T ratio to compensate for small variations in the ankle positioning. Since surgical correction of the T-T ratio following TAR has also been shown to correlate with better clinical results, pain level and ankle range-of-motion [7,10], we believe that the T-T ratio represents an excellent option for sagittal balance evaluation of TAR in the clinical setting, with both radiography and MRI.

We found better repeatability and reliability of the LTS measurements on radiographs than on MRI. Veljkovic et al. described the LTS as a reproducible measure of sagittal talar position [17]. Our study found LTS mean values of 2.96 ± 4.62 mm for radiographs and 0.22 ± 3.93 mm for MRI. Although both LTS measurements would fall within the expected normal range described by Veljkovic et al. [17], the difference would probably be clinically important. We believe that the differences found in the agreements and inter-method measurements could be related to variability in the placement of the circle fitting the talar implant dome, which is needed for LTS measurements on radiographs and MRI. On radiographs, the polyethylene liner is radiolucent and the radiopaque talar implant dome therefore well delineated, whereas on MRI the talar implant and polyethylene liner have similarly low in signal intensity, which hinders the proper visualization of the talar implant dome contour and potentially influences intra- and inter-reader agreements. Besides of this variability, we strongly feel that LTS measurements, in a controlled and systematic approach, represent an important tool for ankle sagittal balance evaluation.

Finally, we found good to excellent intra- and inter-reader agreements for T-L ratio on radiographs and even slightly better on MRI. The lateral process of the talus was first described to be found in line with the axis of the tibia by Paley et al. [4]. Tochigi et al. described the Tibial-axis-to-Lateral Process Distance [13], measured in percentage (T-L ratio), as a potential tool for ankle sagittal balance evaluation. It represented, however, the most sensitive measurement to malpositioning in both transverse and sagittal planes. In our prospectively planned study, we attempted to

Table 3
Intra-class correlations for each measurement in each image type.

Measurement	Radiographs			MR Images		
	Intra-class		Inter-class standard deviation	Concordance		Inter-class standard deviation
	Correlation	95% Interval		Correlation	95% Interval	
LTS	0.886	(0.765, 1.000)	0.917	0.779	(0.573, 0.985)	0.519
T-T Ratio	0.783	(0.580, 0.985)	2.378	0.914	(0.822, 1.000)	0.684
T-L Ratio	0.902	(0.798, 1.000)	0.804	0.936	(0.865, 1.000)	0.456

LTS = Lateral Talar Station.
T-T Ratio = Tibial-axis-to-Talus Ratio.
T-L Ratio = Tibial-axis-to-Lateral Process Distance, normalized to the talar length.

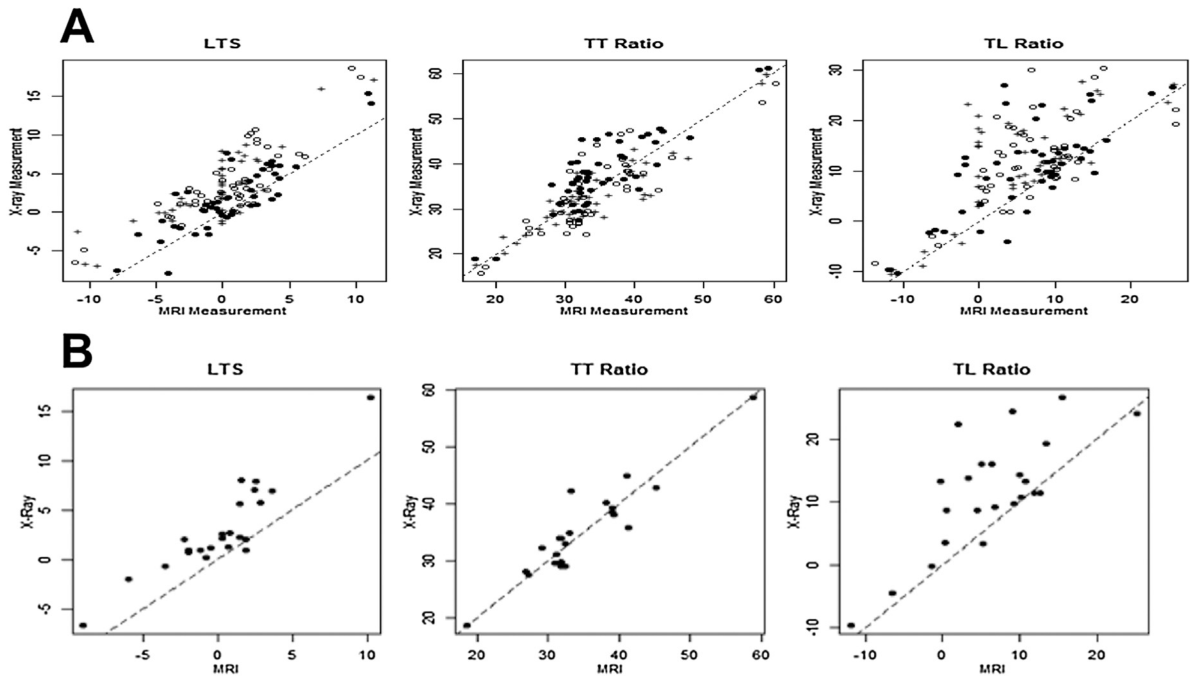

Fig. 8. Concordance and comparability plots of the radiographic and MRI measurements before (A) and after (B) removal of the effects of readers and replication. LTS = Lateral Talar Station. T-T ratio = Tibial-axis-to-Talus ratio. T-L ratio = Tibial-axis-to-Lateral Process distance, normalized to the talar length.

Table 4
Concordance and comparability of the measurements from the two image types.

Measurement	Concordance correlation	95% confidence interval
LTS	0.725	(0.539, 0.843)
T-T Ratio	0.930	(0.842, 0.969)
T-L Ratio	0.616	(0.354, 0.789)

LTS = Lateral Talar Station.
T-T Ratio = Tibial-axis-to-Talus Ratio.
T-L Ratio = Tibial-axis-to-Lateral Process Distance, normalized to the talar length.

control for the positioning of the ankle on radiographs and MRI. We found mean values for T-L distance which were on average within the normal range described by Tochigi et al. [13]. We again found lower values on MRI when compared to radiography. The mean difference was 3.88 mm for T-L distances and 6.25% for T-L ratio, which might be clinically important. Statistical model analysis failed to reveal similarity between radiographic and MRI measurements, suggesting a real difference between the two techniques. While it is unknown which technique is closer to the truth, we believe that due to the projectional nature and difficulties in controlling ankle positioning of radiographs and the better visualization of anatomical landmarks on MRI, T-L ratio and T-L obtained with MRI are more accurate.

Our study has several limitations. First, the number of included subjects was limited. Second, we did not correlate our sagittal balance findings to any specific clinical data. It would be of interest to evaluate this correlation in a prospective study. Third, although we paid meticulous attention to control for malalignment of the ankle during the acquisition of conventional radiographs images using a standardized protocol, alignment variations potentially occurred and influenced the results of our study. Fourth, we performed measurements on weight-bearing radiographs and non-weight-bearing MR images. Despite the semi-constrained design of the total ankle replacement implant in all subjects, the weight load during radiography may have influenced the outcomes of our study. Fifth, all subjects included in our study had the same semi-constrained TAR implant. Results may vary with other implants, specifically mobile-bearing designs, where anterior talar translation could occur during non-weight-bearing MR image acquisition. Sixth, while we were able to determine reliability, repeatability and difference of radiography and MRI measurements, we do not know which measurements are more accurate in reflecting the true sagittal balance. A quantitative cadaver study could be a means to find out which technique is most accurate. Finally, as we did not include coronal plane alignment assessments in our study, the performance of MARS MRI for the evaluation of coronal plane malpositioning of replaced ankles is currently unknown.

In conclusion, sagittal balance measurements performed on standardized WB radiographs and MARS MRI demonstrate substantial correlation and similarity. Given its high inter- and intra-observer agreement, MARS MRI may be helpful for the evaluation of sagittal balance following total ankle replacements. Our results allow us to recommend the use of MARS MRI as a good and reliable alternative for TAR sagittal balance evaluation.

Conflicts of interest statement

This work was supported by an institutional grant from Siemens Healthcare USA, which provided funding for the MRI exams and remuneration for study participants. The decision to recruit the proper subjects who meet the criteria was based on clinical presentation and decided by the orthopaedic surgeon.

References

[1] McKellop H.A., Llinas A, Sarmiento A. Effects of tibial malalignment on the knee and ankle. Orthop Clin North Am 1994;25:415–23.
[2] Ting AJ, Tarr RR, Sarmiento A, Wagner K, Resnick C. The role of subtalar motion and ankle contact pressure changes from angular deformities of the tibia. Foot Ankle 1987;7:290–9.
[3] Tarr RR, Resnick CT, Wagner KS, Sarmiento A. Changes in tibiotalar joint contact areas following experimentally induced tibial angular deformities. Clin Orthop Relat Res 1985;72–80.
[4] Paley D, Herzenberg JE, Tetsworth K, McKie J, Bhave A. Deformity planning for frontal and sagittal plane corrective osteotomies. Orthop Clin North Am 1994;25:425–65.

[5] Wood PL, Sutton C, Mishra V, Suneja R. A randomised, controlled trial of two mobile-bearing total ankle replacements. J Bone Joint Surg Br 2009;91:69–74.
[6] Barg A, Elsner A, Chuckpaiwong B, Hintermann B. Insert position in three-component total ankle replacement. Foot Ankle Int 2010;31:754–9.
[7] Braito M, Dammerer D, Reinthaler A, Kaufmann G, Huber D, Biedermann R. Effect of coronal and sagittal alignment on outcome after mobile-bearing total ankle replacement. Foot Ankle Int 2015;36:1029–37.
[8] Conti SF, Wong YS. Complications of total ankle replacement. Clin Orthop Relat Res 2001;105–14.
[9] Hintermann B, Valderrabano V, Dereymaeker G, Dick W. The HINTEGRA ankle: rationale and short-term results of 122 consecutive ankles. Clin Orthop Relat Res 2004;57–68.
[10] Lee YS, Lee BK, Lee SH, Park HG, Jun DS, Moon DH. Effect of foot rotation on the mechanical axis and correlation between knee and whole leg radiographs. Knee Surg Sports Traumatol Arthrosc 2013;21:2542–7.
[11] Myerson MS, Mroczek K. Perioperative complications of total ankle arthroplasty. Foot Ankle Int 2003;24:17–21.
[12] Pyevich MT, Saltzman CL, Callaghan JJ, Alvine FG. Total ankle arthroplasty: a unique design. Two to twelve-year follow-up. J Bone Joint Surg Am 1998;80:1410–20.
[13] Tochigi Y, Suh JS, Amendola A, Saltzman CL. Ankle alignment on lateral radiographs. Part 2: reliability and validity of measures. Foot Ankle Int 2006;27:88–92.
[14] de Cesar Netto C, Fonseca LF, Fritz B, Stern SE, Raithel E, Nittka M, Schon LC, Fritz J. Metal artifact reduction MRI of total ankle arthroplasty implants. Eur Radiol 2018;28(5)2216–27, doi:http://dx.doi.org/10.1007/s00330-017-5153-9 Epub 2017 Dec 7.
[15] Kumar NM, de Cesar Netto C, Schon LC, Fritz J. Metal artifact reduction magnetic resonance imaging around arthroplasty implants: the negative effect of long echo trains on the implant-related artifact. Invest Radiol 2017;52:310–6.
[16] Fritz J, Ahlawat S, Demehri S, Thawait GK, Raithel E, Gilson WD, et al. Compressed sensing SEMAC: 8-fold accelerated high resolution metal artifact reduction MRI of cobalt-chromium knee arthroplasty implants. Invest Radiol 2016;51:666–76.
[17] Veljkovic A, Norton A, Salat P, Saltzman C, Femino J, Phisitkul P, et al. Lateral talar station: a clinically reproducible measure of sagittal talar position. Foot Ankle Int 2013;34:1669–76.
[18] Albert TJ, Sharkey PF, Chao W, Hume EL, Rothman RH. Rotation affects apparent radiographic positioning of femoral components in total hip arthroplasty. J Arthroplasty 1991;6(Suppl):S67–71.
[19] Eckrich SG, Noble PC, Tullos HS. Effect of rotation on the radiographic appearance of the femoral canal. J Arthroplasty 1994;9:419–26.
[20] Goodman S, Rubenstein J, Schatzker J, Kadish L, Fornasier V. Apparent changes in the alignment of the femoral component in hip arthroplasties associated with limb positioning. Clin Orthop Relat Res 1987;242–5.
[21] Ivarsson I, Myrnerts R. The effect of the radiographic projection on the measured position of the prosthesis at knee arthroplasty. Arch Orthop Trauma Surg 1986;105:350–2.
[22] Sabharwal S, Zhao C. Assessment of lower limb alignment: supine fluoroscopy compared with a standing full-length radiograph. J Bone Joint Surg Am 2008;90:43–51.
[23] Stehle J, Moore SM, Alaseirlis DA, Debski RE, McMahon PJ. Acromial morphology: effects of suboptimal radiographs. J Shoulder Elbow Surg 2007;16:135–42.
[24] Haskell A, Mann RA. Ankle arthroplasty with preoperative coronal plane deformity: short-term results. Clin Orthop Relat Res 2004;98–103.
[25] Wood PL, Prem H, Sutton C. Total ankle replacement: medium-term results in 200 Scandinavian total ankle replacements. J Bone Joint Surg Br 2008;90:605–9.
[26] Saltzman CL, Tochigi Y, Rudert MJ, McIff TE, Brown TD. The effect of agility ankle prosthesis misalignment on the peri-ankle ligaments. Clin Orthop Relat Res 2004;137–42.
[27] Anderson T, Montgomery F, Carlsson A. Uncemented STAR total ankle prostheses: Three to eight-year follow-up of fifty-one consecutive ankles. J Bone Joint Surg Am 2003;85-A:1321–9.
[28] Kopp FJ, Patel MM, Deland JT, O'Malley MJ. Total ankle arthroplasty with the Agility prosthesis: clinical and radiographic evaluation. Foot Ankle Int 2006;27:97–103.
[29] Cenni F, Leardini A, Cheli A, Catani F, Belvedere C, Romagnoli M, et al. Position of the prosthesis components in total ankle replacement and the effect on motion at the replaced joint. Int Orthop 2012;36:571–8.
[30] Coetzee JC, Castro MD. Accurate measurement of ankle range of motion after total ankle arthroplasty. Clin Orthop Relat Res 2004;27–31.
[31] Tochigi Y, Rudert MJ, Brown TD, McIff TE, Saltzman CL. The effect of accuracy of implantation on range of movement of the Scandinavian total ankle replacement. J Bone Joint Surg Br 2005;87:736–40.
[32] Kohonen I, Koivu H, Pudas T, Tiusanen H, Vahlberg T, Mattila K. Does computed tomography add information on radiographic analysis in detecting periprosthetic osteolysis after total ankle arthroplasty. Foot Ankle Int 2013;34:180–8.
[33] Mason LW, Wyatt J, Butcher C, Wieshmann H, Molloy AP. Single-photon-emission computed tomography in painful total ankle replacements. Foot Ankle Int 2015;36:635–40.
[34] Magerkurth O, Frigg A, Hintermann B, Dick W, Valderrabano V. Frontal and lateral characteristics of the osseous configuration in chronic ankle instability. Br J Sports Med 2010;44:568–72.